Climatic Change
https://doi.org/10.1007/s10584-020-02736-z

Land use changes in Southeastern Amazon and trends in rainfall and water yield of the Xingu River during 1976–2015

Rodnei Rizzo[1] · Andrea S. Garcia[1] · Vívian M. de F. N. Vilela[1] · Maria Victoria R. Ballester[1] · Christopher Neill[2] · Daniel C. Victoria[3] · Humberto R. da Rocha[4] · Michael T. Coe[2]

Received: 13 May 2019 / Accepted: 6 May 2020/

Abstract
Since the early 1970s, the agricultural frontier of southeastern Amazon has undergone extensive land use changes. These alterations, combined with regional climate changes, have the potential to influence the hydrologic cycle at small to large scales. We evaluated a 40-year time series (1976 to 2015) of rainfall and water yield and related them to land use changes in the Upper Xingu River Basin (UX). We acquired data from six rainfall stations and four river gauges and mapped land use changes. Mann-Kendall trend analysis and Pettitt's change point detection were employed to describe annual and seasonal changes in the time series. Monthly water yield from the Xingu River was used to derive annual, seasonal, and monthly water yield, as well as the runoff coefficient. The largest changes in land use occurred during the last two decades and approximately 60,900 km^2 in the Upper Xingu Basin were deforested between 1985 and 2015. Rainfall in the Xingu Basin decreased by about 245 mm over the period but there was no trend in water yield. The number of rainy days and intensity of events also decreased, but the length of the rainy season and seasonal and annual water yield did not change. Although watershed deforestation has increased water yield in other Amazon rivers, the reduction in rainfall in the Upper Xingu Basin was high enough to mask this effect.

Keywords Amazônia · Upper Xingu Basin · Deforestation · Land use changes · Climate change · Mann-Kendall analysis · Hydro-climatological indicators

1 Introduction

Since the early 1970s, large portions of Amazon have experienced rapid and widespread deforestation associated with the expansion of the agricultural frontier (Morton et al. 2006;

✉ Maria Victoria R. Ballester
vicky@cena.usp.br

Extended author information available on the last page of the article

DeFries et al. 2013; Garcia et al. 2017). However, since the 1990s, increasing food demands from international markets have become a main driver of forest change. Recent land use change in southern Amazônia has been characterized by expansion of both croplands and pastures, a shift to expansion of croplands into pasturelands (Macedo et al. 2012) and intensification and double-cropping (Spera et al. 2016).

The combined effects of forest loss and climate changes have altered the energy and water balances (Panday et al. 2015; Silvério et al. 2015). The Amazon forest plays a critical role in the water and energy cycles. Trees can draw on water from eight meters or more in the soil, which supplies water even during intense dry seasons (Panday et al. 2015). High year-round evapotranspiration (ET) returns a large volume of water to the atmosphere. Forest cover loss reduces ET and increases sensible heat flux (Silvério et al. 2015), thus reducing humidity, cloud formation, and rainfall (Wright et al. 2017). At the scale of small watersheds, reduced evapotranspiration following deforestation increases runoff in small streams by three- to four-fold (Hayhoe et al. 2011). Changes at larger scales are often less dramatic, but studies suggest that discharge has been increased by as much as 20%, because of land use change (Costa et al. 2003; Júnior et al. 2015) or a combination of land use and interdecadal variations in the regional climate (Coe et al. 2011; Levy et al. 2018). Others have suggested that secondary growth of vegetation and climate change have attenuated the increase in discharge (Von Randow et al. 2019). Decreased rainfall caused by forest loss could result in lower river flows (Spracklen et al. 2012). These feedbacks among changes to land cover, water balance, and climate have the potential to reduce precipitation, increase precipitation variability, and threaten agricultural production, energy production, and regional communities whose livelihood depends on freshwater resources.

The Xingu River is a large, southern Amazon River tributary that lies within a zone of highly seasonal rainfall that is dominated by soils suitable for crop agriculture. The Xingu Basin experienced large alterations in land cover between 2000 and 2010. Approximately 12% of the Basin (or 19,000 km^2) was deforested after 2000, despite the presence of large protected forest areas in the central Basin (Silvério et al. 2015). The Xingu Basin is now one of the Brazil's most important agricultural regions and produces 13% of Brazil's soybeans, most of which is exported to Asia and Europe (Lathuillière et al. 2014).

Because of large and recent changes in land cover within the time frame of historical rainfall and river flow instrument records, the upper Xingu Basin provides an opportunity to evaluate relationships between land cover and changes to the hydrologic cycle. Evaluating changes to rainfall and water yield (river discharge per unit of area) is essential to understand how the combined effect of anthropogenic activities and global climate change have altered freshwater resources and how these changes might affect other important areas of current or future agricultural expansion. This study addresses the following questions: (a) How has rainfall in the upper Xingu changed during the last 40 years (1976 to 2015)? and (b) do the water yield of the Xingu River and its tributaries also changed?

2 Materials and methods

2.1 Study site and datasets

The Xingu Basin lies in the states of Mato Grosso and Pará, within the southern Amazon's "arc of deforestation." The area is located between latitude 7.5°S and 15°S

and longitude 51°W and 55.5°W. The 210,000-km^2 Basin includes the highly deforested headwater region and a less altered lower central Xingu Basin (Fig. 1). Originally covered by transitional forests (about 80% of the area), the area encompasses the central Brazil Cerrado (savanna) and more humid forests to the north. Precipitation is heterogeneously distributed through the year, with an average annual value of 1900 mm year^{-1} (Hayhoe et al. 2011). A dry season typically lasts from May to August and a wet season from September to April (Marengo et al. 2011).

To examine changes to river flows at the scale of the upper Xingu Basin, we compiled data of monthly river discharge from two gauges from the Brazilian National Water Agency database (Table 1). Gauge 1 was located in the municipality of São Jose do Xingu (Fig. 1, gauge 1) and measures the discharge generated by the entire study Basin. The discharge record for this station was from 1976 to 2015. We also acquired data from a tributary in the Upper Xingu Basin, the Ronuro River, which had a long and consistent discharge record (Fig. 1, gauge 2). To evaluate how the land use change influenced stream discharge at the scale of small watersheds with nearly homogeneous land use, we compiled hourly discharge measurements for the last 10 years (2007 to 2017) (Table 1), from one small forest watershed and one small cropland watershed at Tanguro Ranch using a record that was initiated by Hayhoe et al. (2011) (Fig. 1, gauges 3 and 4). Once all discharge data was gathered, such information was converted to water yield (discharge per unit of area). This conversion intended to make rainfall and river flow data units comparable, facilitating the analysis and discussion.

Data from 59 rainfall stations were organized according to water years (12 months ranging from September to August of the following year). Years with more than 36 total days of missing data or more than 10 consecutive days of missing data were removed from the analysis. Then, a data quality control (QC) was performed to reduce errors from technical sources. The QC procedure worked on an annual time step and compared each station and its neighbors, looking for abnormal differences (Delahaye et al. 2015). For each station, 14 indicators were calculated and used to identify years with data inconsistencies. We restricted our analysis to stations that covered 1976 to 2015 with less than 11 non-consecutive missing years. Six stations met the QC's criteria and were selected for further analysis. Finally, precipitation data were averaged to create a 40-year time series of daily rainfall.

2.2 Land use change

We used Landsat images acquired from USGS/Landsat Higher Level Science Data Products for the years 1985, 1990, 1995, 2000, 2005, 2010, and 2015. All images corresponded to the dry season and ranged from Julian day 154 to 220. For each year, 30-m spatial resolution images of either LANDSAT 5, LANDSAT 7, or LANDSAT 8 were classified. Additionally, croplands were defined with a smoothed satellite time series of MODIS Vegetation Indices, from the Institute of Surveying, Remote Sensing, and Land Information (University of Natural Resources and Life Science, Vienna). The temporal and spatial scales of this product were 8 days and 250 m, respectively.

Images were mosaicked and geometrically corrected with root mean square error (RMSE) lower than 15 m (i.e., 0.5 pixel). Later, mosaics were classified according to Garcia et al. (2019). First, natural or semi-natural areas were extracted by an ISODATA algorithm, in which each resulting class was reclassified into forest, woody vegetation, grassland, secondary

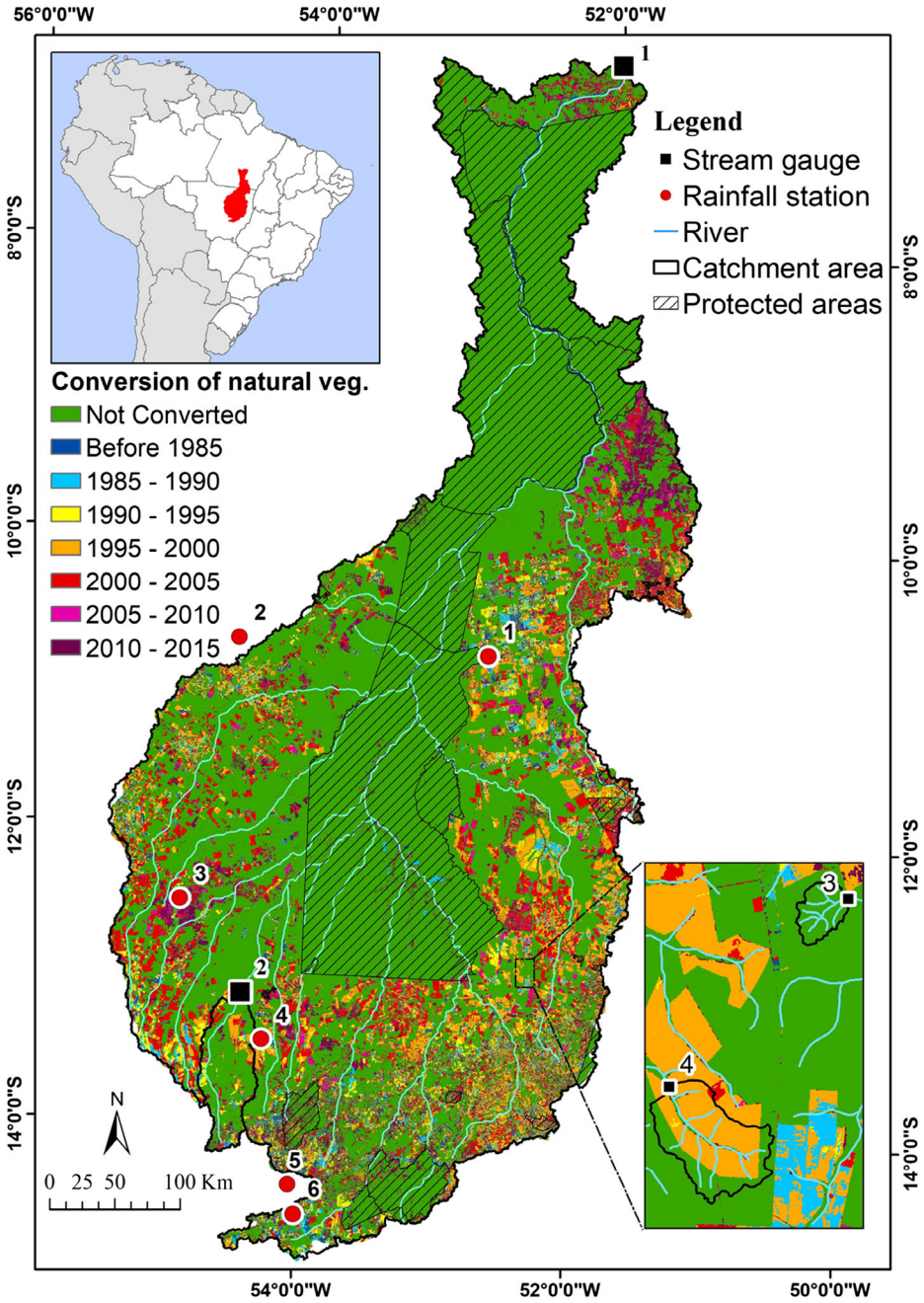

Fig. 1 The Xingu Basin, showing agricultural areas by year of conversion and location of rainfall stations and river gauges

complex, agriculture, water surface, bare soil, and burned land. Then, MODIS temporal profiles were used to identify managed areas and classify them into pasturelands or croplands (Arvor et al. 2011).

Table 1 Description of rainfall stations, river gauges, and the results of trend analysis for annual data

Id	Station	Long °	Lat.	Period	Catchment area (km²)
Rainfall station					
1	S.J.do Xingu	− 52.75	− 10.81	1976–2011	–
2	Cajabi	− 54.55	− 10.75	1976–2015	–
3	Rio Ferro	− 54.19	− 12.51	1976–2013	–
4	Agrochapada	− 54.28	− 13.45	1976–2011	–
5	Paranatinga	− 54.05	− 14.42	1976–2015	–
6	BR-309	− 53.99	− 14.61	1976–2015	–
River gauges					
1	Xingu River	− 51.99	− 6.73	1976–2015	210,359
2	Ronuro River	− 54.44	− 13.14	1976–2007	3845
3	Stream Forest	− 52.33	− 12.83	2007–2017	6.73
4	Stream Soy	− 52.43	− 12.54	2007–2017	27.53

2.3 Hydro-climatological indicators

To examine patterns in the long-term datasets, we derived a group of annual hydro-climatological indicators from the precipitation and water yield data. The wet season onset and end dates were defined based on the average precipitation time series, following Arvor et al. (2014):

$$\mathrm{AA}(t) = \sum_{n=1}^{t} \left(R(n) - \overline{R} \right) \tag{1}$$

where AA(t) represents the anomalous accumulation at day t, $\overline{R}$ is the average daily rainfall, and $R(n)$ is the daily rainfall at day n. The rainy season onset and end were then determined by the minimum and maximum of AA. We also derived the average period of consecutive days without precipitation (d_{mean}), average period of consecutive days with precipitation (w_{mean}), percentage of rain events higher than 1 mm ($\mathrm{nb1_p}$), 10 mm ($\mathrm{nb10_p}$), 20 mm ($\mathrm{nb20_p}$), and 50 mm ($\mathrm{nb50_p}$).

We used the following indicators to describe variations in river flows: annual water yield ($\mathrm{wy_a}$), dry season (Jun–Sep) water yield ($\mathrm{wy_{ds}}$), wet season (Oct–May), water yield ($\mathrm{wy_{WS}}$), lowest monthly water yield ($\mathrm{wy_{LM}}$), highest monthly water yield ($\mathrm{wy_{hm}}$), and the ratio between annual discharge and annual rainfall, or runoff coefficient (RC).

2.4 Trend analysis and change point detection

We submitted time series of rainfall, water yield, and the derived indexes to Mann-Kendal trend test (MK) (Mann 1945; Kendall 1975). The technique defines if a variable consistently changes through time or has an increasing or decreasing trend. Before applying the MK test, we evaluated the serial correlation of the datasets and, if necessary, employed a trend-free pre-whitening (TFPW) method to eliminate adverse effects (Yue et al. 2002).

The MK test started by applying an indicator function (sgn) on the difference between all possible pairs of measurements (Eq. 2). The value measured in time j (xj) was subtracted from the values previously observed (xi), considering that time $j > i$. Then, these differences were used to define Kendall's statistics S (Eq. 3):

$$sgn(\theta) = \begin{cases} +1 \\ 0 \quad if \\ -1 \end{cases} \begin{bmatrix} \theta > 0 \\ \theta = 0 \\ \theta < 0 \end{bmatrix} \tag{2}$$

$$S = \sum_{i=1}^{n-1} \sum_{j=i+1}^{n} sgn\left(x_j - x_i\right) \tag{3}$$

where n is the length of the dataset. Based on S, the variance $V(S)$ (Eq. 4) and the normalized test statistics Z (Eq. 5) were calculated:

$$Z = \begin{cases} \dfrac{S-1}{\sqrt{V(S)}} & if S > 0 \\ 0 & if S = 0 \\ \dfrac{S+1}{\sqrt{V(S)}} & if S < 0 \end{cases} \tag{4}$$

$$V(S) = \frac{1}{18}[n(n-1)(2n+5)] \tag{5}$$

where the null hypothesis of no trend was rejected, if the absolute value of Z was higher than the theoretical value of $Z(1\text{-}\alpha/2)$ (at 0.05 level of significance). A positive S value indicated an increasing trend while a negative S indicates a decreasing trend. The magnitude of the trend was represented by the Sen's slope (Sen 1968) calculated over the time period.

We used the Pettitt test (Pettitt 1979), a nonparametric method, capable of detecting changes in the time series mean, to identify abrupt changes in the time series. The test performs a rank-based comparison between the subsets $k(\tau)$ (Pettitt 1979; Zhang et al. 2015):

$$k(\tau) = \sum_{i=1}^{\tau} \sum_{j=\tau+1}^{n} sgn\left(x_j - x_i\right) \tag{6}$$

where *sgn* corresponds to Eq. 2. The abrupt change was defined as the date τ where the absolute value of $k(\tau)$ is the maximum. The p value of the statistical test was then computed using the approximated limiting distribution by Pettitt (Pettitt 1979).

3 Results

3.1 Land use change

The Xingu Basin experienced high rates of deforestation and conversion to agriculture from 1985 to 2015 (Fig. 1). In 1985, native forests and Cerrado covered 199,500 km^2, approximately 95% of the Basin (Fig. 2a). From 1985 to 2015, 60,900 km^2 (29% of the Basin) was converted into pastures and croplands. The highest conversion rates occurred between 1995 and 2005, when 36,000 km^2 of native vegetation was converted (Fig. 2a). Land use changes were most concentrated in the central east and southern regions of the Basin, while a large area of intact tropical forest, in the Xingu Indigenous Park, remains in the central portion of the Basin (Fig. 1). Pasture area increased three-fold between 1985 and 2015, covering about

32,000 km^2 in 2015. In contrast, croplands were nearly nonexistent in 1985 but covered about 23,000 km^2 in 2015. Highest rates of native vegetation conversion to pastures took place between 1995 and 2000 (about 17,000 km^2), while cropland expansion was greater between 2000 and 2015 (about 21,000 km^2). The pattern of land use change in the Ronuro River Basin was nearly identical to that in the entire Basin (Fig. 2b).

3.2 Rainfall trends

The Mann-Kendall test of each rainfall station showed significant downward trends for four stations, negative S in all cases, and p values ranged from 0.001 to 0.35 (Table 2). Sen's slope indicated rainfall reductions of 10 to 25 mm year^{-2}. Although not significant, the trends from Rio Ferro and Cajabi stations were also downward (Table 2).

An average time-series was calculated from the six stations to facilitate the evaluation of the rainfall temporal changes. The average values provide a better representation of the variation over the entire Basin (Fig. 1). The average annual rainfall calculated from the six stations also indicated a downward trend, with a slope of 12.7 mm year^{-2} (Fig. 3a). Rainy season rainfall decreased by 10.4 mm year^{-2} (Fig. 3b) and dry season rainfall decreased 1.2 mm year^{-2} (Fig. 3c). Both seasonal and annual values changed abruptly about 1996. Before 1996, the average annual rainfall was 1900 mm in the wet season and 85 mm in the dry season. After 1996, these values were 1700 mm and 40 mm. The difference in annual rainfall averages, before

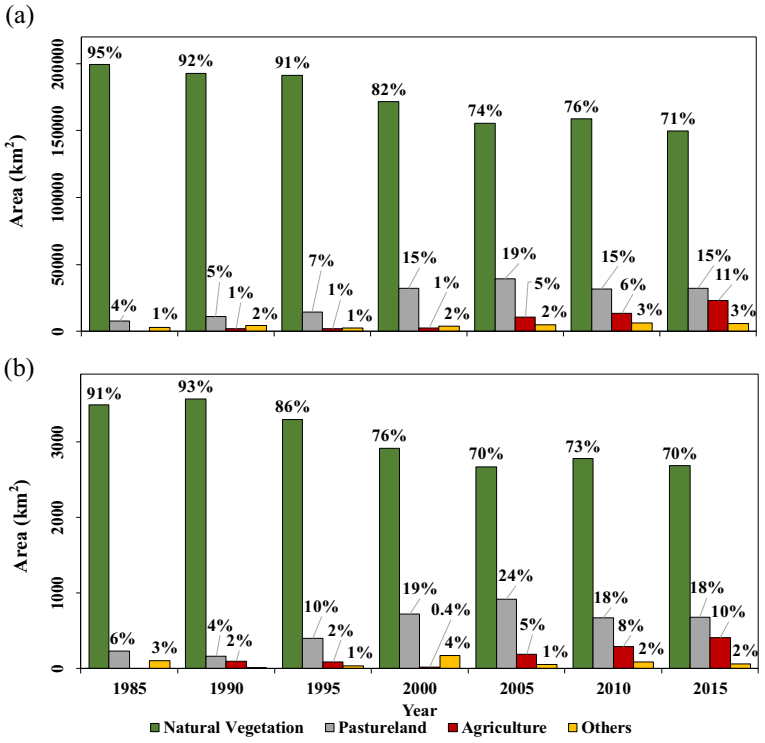

Fig. 2 Land use changes in entire Xingu Basin (**a**) and in the catchment at Ronuro River (**b**), for the period of 1985–2015

Table 2 Trend analysis for annual data of each rainfall station

Id	Station	*S*	Sen's slope (mm year^{-2})	*p* value	Available data (%)
1	S.J.do Xingu	−0.31	−15.19	0.01	81
2	Cajabi	−0.12	−7.33	0.35	73
3	Rio Ferro	−0.23	−11.03	0.08	74
4	Agrochapada	−0.26	−9.74	0.04	84
5	Paranatinga	−0.4	−9.56	0.001	73
6	BR-309	−0.43	−25.91	0.001	78

and after the abrupt change, was 245 mm (Fig. 3). The change coincided with an abrupt increase in the deforested area in the upper Xingu Basin (Figs. 2 and 3).

The indexes representing the percentage of rainy days with rain > 1, 10, 20, and 50 mm (nb_{1p}, nb_{10p}, nb_{20p}, nb_{50p}) all had downward trends. Mann-Kendall test indicated an average decrease of 16 days (0.11% year^{-2}) in the number of days with events > 1 mm during the rainy seasons from 1976 to 2015, and gaps between two rain events increased on average 1 day. Events in the dry season also changed. The nb_{1p} decreased by 3 days (0.06% year^{-2}) and nb_{10p}

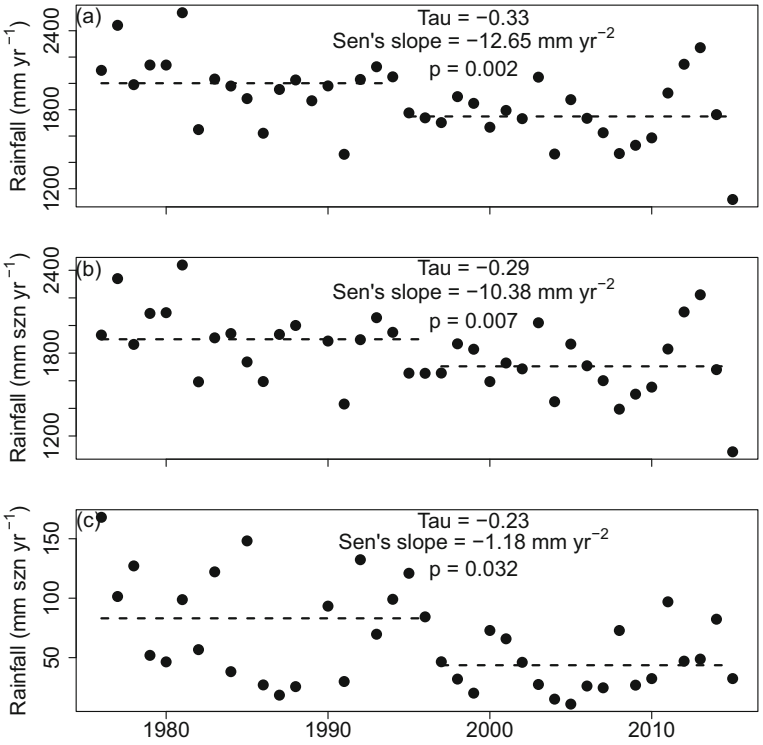

Fig. 3 Annual (**a**), wet (**b**), and dry season (**c**) rainfall and the corresponding parameters of the Mann-Kendall trend analysis. Dotted lines represent the average rainfall of periods before and after abrupt change

decreased 1 day (0.02% year^{-2}). In some cases, such changes were not linear but rather changed abruptly. The Pettitt test detected abrupt changes in the number of consecutive days with precipitation, as well as the number of rain events greater than 1 mm and 10 mm (Table 3). Such results were detected for annual and wet season indicators, while the only dry season indicator with an abrupt change was nb_{1p}. These changes were all observed between 1989 and 1994.

Although rainfall amounts changed over time, there were no changes to the total length of the wet and dry seasons (Table 3). There was also no significant change ($p > 0.05$, Table 3) to the average rainy season onset date (October 20th, day 50 of the hydrologic year) or end date (March 20th, day 230 of the hydrological year) (Fig. 4).

3.3 Water yield trends

The longest available time series from small (7 to 28 km^2) single land-use catchments in forest or cropland showed that average monthly water yield was 48.99 mm month^{-1} in the cropland catchment (Fig. 5) while in forest, it corresponded to 18.40 mm month^{-1}. In addition to higher water yield, flow varied more in the cropland catchment (Fig. 5).

Table 3 Trend analysis of rainfall indicators derived from averaged annual and seasonal data from upper Xingu Basin

MK analysis	Onset	End	d_{mean}[a]	w_{mean}[b]	nb_{1p}[c]	nb_{10p}[d]	nb_{20p}[e]	nb_{50p}[f]
Annual								
S	–	–	0.18	−0.28	−0.24	−0.36	0.31	−0.25
Sen's slope[g]	–	–	0.13	−0.01	−0.11	−0.10	−0.06	−0.019
p	–	–	0.10	0.010	0.029	0.001	0.004	0.021
Pettitt test	–	–	1989	1988	1988	1994	1994	1981
μ_{aac}-μ_{bac}[h]	–	–	4.18	−0.59	−3.17	−2.25	−1.03	−2.01
p	–	–	−0.250	0.012	0.048	0.008	0.070	0.25
Wet season								
S	0.10	0.13	0.24	−0.29	−0.21	−0.33	−0.30	−0.23
Sen's slope[g]	0.16	0.24	0.027	−0.01	−0.12	−0.14	−0.09	−0.02
p	0.365	0.187	0.027	0.007	0.051	0.002	0.006	0.036
Pettitt test	1991	1981	1997	1989	1989	1994	1994	1982
μ_{bac}-μ_{aac}[h]	6.10	6.91	0.65	−0.52	−4.27	−2.82	−1.33	−0.43
p	0.506	0.368	0.206	0.015	0.039	0.001	0.098	0.14
Dry season								
S	–	–	0.16	−0.21	−0.28	−0.24	−0.13	–
Sen's slope[g]	–	–	0.24	−0.004	−0.06	−0.02	−0.009	–
p	–	–	0.133	0.050	0.011	0.03	0.22	–
Pettitt test	–	–	1991	1985	1996	1986	1986	–
μ_{bac}-μ_{aac}[h]	–	–	8.2	−0.21	−1.59	−0.555	−0.219	–
P	–	–	0.226	0.065	0.03	0.076	0.453	–

[a] Average period of consecutive days without precipitation

[b] Average period of consecutive days with precipitation

[c] Percentage of rain events > 1 mm

[d] > 10 mm

[e] > 20 mm

[f] > 50 mm

[g] Slope unit to onset, end, d_{mean}, w_{mean} is days year^{-1} and unit to nb_{1p}, nb_{10p}, nb_{20p}, nb_{50p} is % year^{-1}

[h] Difference between means after (μ_{bac}) and before (μ_{bac}) abrupt change

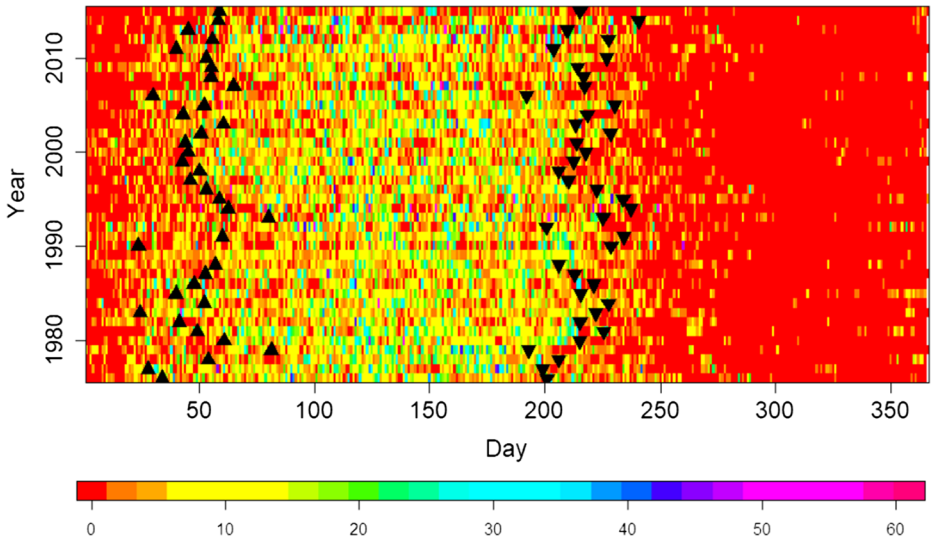

Fig. 4 Average daily rainfall in millimeters, onset (▲) and end (▼) dates derived from the time series. Rainfall values were calculated averaging the daily information from the available stations in the Xingu Basin

Trend analysis of Ronuro river data indicated an annual water yield decrease of 4.2 mm year^{-2} (Table 4). Highest and lowest monthly water yield also had downward trends of 0.75 mm month year^{-1} and − 0.1 mm moth year^{-1} (Table 4), respectively. Similarly, dry season water yield decreased by 3.5 mm szn year^{-1} (Table 4), while there was no trend in the wet season. Annual water yield, as well as water yield in the dry season, and water yield in the month of lowest rainfall all changed abruptly between 1995 and 1997. The difference between means after and before the change corresponded to − 83.5 mm (annual), − 25.39 mm (in dry season), and − 3.32 mm (in month of lowest rainfall).

In the Xingu Basin, lowest monthly water yield was the only metric with a significant trend (− 0.07 mm month year^{-1}; 24%) (Table 4). This metric also changed abruptly 1997, with an average value of 12.64 mm year^{-1} before and 10.44 mm year^{-1} after this date. Although no trend was detected in Xingu water yield, the Pettitt test indicated a significant abrupt change in 1995. Usually, variations in climate are not linear; consequently, periodic oscillation is

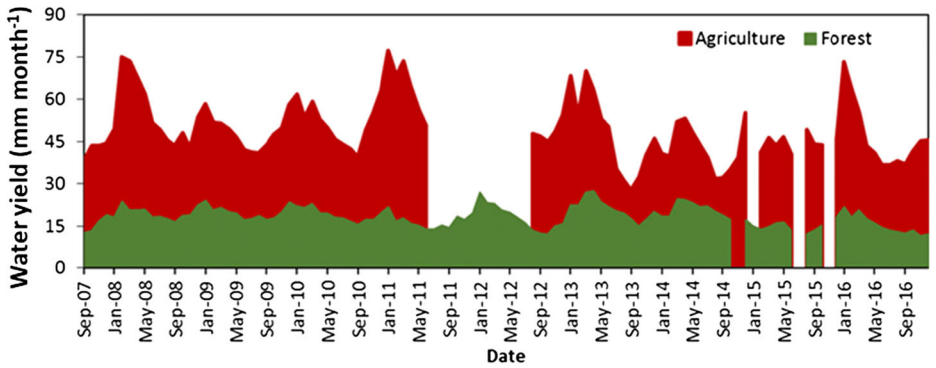

Fig. 5 Monthly water yield in forested and soybean cropland catchments located at Tanguro Ranch in the southeastern Xingu Basin

Table 4 Trend and abrupt change analyses derived from hydrological indexes μ_{aac}-μ_{bac}

Index	*S*	Sen's slope	*p*	Pettitt test	μ_{aac}-μ_{bac}[g]	*p*
Ronuro River						
wy_a[a]	−0.31	−4.25	0.01	1995	83.57	0.05
wy_{lm}[b]	−0.24	−0.1	0.05	1997	−3.32	0.05
wy_{ds}[c]	−0.28	−3.46	0.02	1997	−25.39	0.02
wy_{hm}[d]	−0.23	−0.75	0.06	1985	−23.36	0.14
wy_{ws}[e]	−0.15	−0.74	0.23	1985	−69.63	0.08
C[f]	−0.12	−0.11	0.32	1996	−0.008	0.36
Xingu River						
wy_a[a]	−0.17	−1.6	0.11	1995	−58.02	0.03
wy_{lm}[b]	−0.32	−0.07	0.003	1997	−1.87	< 0.0001
wy_{ds}[c]	−0.13	−0.5	0.22	1997	−20.55	0.16
wy_{hm}[d]	−0.1	−0.28	0.35	1983	−20.46	0.66
wy_{ws}[e]	−0.17	−1.28	0.12	1995	−39.18	0.1
C[f]	0.15	0.12	0.17	2003	0.044	0.058

[a] Annual water yield (wy_a) (mm $year^{-2}$)

[b] Lowest month water yield (wy_{lm}) (mm month $year^{-1}$)

[c] Dry season water yield (wy_{ds}) (mm szn $year^{-1}$)

[d] Highest month water yield (wy_{hm}) (mm month $year^{-1}$)

[e] Wet season water yield (wy_{ws}) (mm szn $year^{-1}$)

[f] Runoff coefficient (C)

[g] Difference between means after (μ_{bac}) and before (μ_{bac}) abrupt change

frequently observed. If no significant trends were observed in the time series, the change detected by Pettitt test might be related to the oscillation of the time series. Furthermore, because higher rates of deforestation should lead to higher streamflow if rainfall does not change, we expected an upward trend in the highest monthly water yield and runoff coefficient.

4 Discussion

4.1 Deforestation and trends in rainy season length

Our finding that rainy season onset and end dates in the upper Xingu Basin have not changed despite high deforestation differed from other studies in literature. Arvor et al. (2017) found a consistent decrease in the southern Amazon's rainy season caused by a delayed rainy season onset. Analysis of daily rainfall from Rondônia suggested that deforestation since the 1970s caused an 18-day delay in the onset of the rainy season (Butt et al. 2011). Leite-Filho et al. (2019) isolated the influence from deforestation in rainfall time-series from 112 stations of southern Amazon and found a delay in the onset of 0.12–0.17 days for each percent increase in deforestation. The authors also described higher probabilities of delayed rainy season onset and longer dry spell events in highly deforested areas. Tropical forest has high capacity to absorb solar radiation and convert this energy in latent heat (da Rocha et al. 2004). When forests are converted to another land use, net radiation (Rn) declines and a higher proportion of Rn is dissipated as sensible heat (Costa and Foley 1997; Bruijnzeel 2004; Coe et al. 2016). The mechanism for the effect is that latent heat flux over the land surface is an important source of

atmospheric humidity during the initial stages of transition between wet and dry seasons (Fu and Li 2004) and deforestation reduces latent heat flux, creates drier conditions in the troposphere, and delays the rainy season's onset (Schubert et al. 2004). Because a delayed rainy season onset caused by deforestation has been found in the range of latitudes 3° to 15°S (Butt et al. 2011; Fu et al. 2013; Debortoli et al. 2016; Wright et al. 2017; Leite-Filho et al. 2019), we expected it for the Xingu, which lies between 10 and 15° S latitude.

Although the forest influences rainfall generation, rainy season length is not exclusively influenced by deforestation (Makarieva et al. 2013). The high variability of onset dates is also related to pre-seasonal conditions in the Pacific Ocean and South American continent (Yin et al. 2014; Arvor et al. 2017), which modulate moisture availability, atmospheric instability, and atmospheric circulation in both low and upper levels (Arvor et al. 2017). Rainy season duration is the result of interactions between local circulation, convective activity from South Atlantic Convergence Zone, and large-scale atmospheric circulation (Negri et al. 2000; Siqueira et al. 2004; Debortoli et al. 2015). Marengo et al. (2012) argue the large variability and uncertainty concerning the onset data trends result from the complex mechanisms that determine the establishment of the monsoon in South America. Considering that variability of onset and end dates has important implications for the analysis of long-term trends (Arvor et al. 2017), these factors likely confounded detection of any change in rainy season length related to the upper Xingu land cover change alone.

4.2 Changes in rainy events, seasonal and annual accumulated precipitations

Although we did not find changes in rainy season onset dates, MK analysis indicated an abrupt reduction in the number of days with precipitation events after 1995 and a 245 mm year^{-1} reduction in the Basin's annual rainfall. These results coincided with high rates of deforestation across the entire southeast Amazon during the 1990s (Pfaff et al. 2007). Abrupt decreases in rainfall in the late 1990s were also found in other locations in the southern Amazon (Debortoli et al. 2015). Reduced rainfall associated with deforestation has also been documented in northwest Rondônia, Brazil (Butt et al. 2011; Spracklen et al. 2012; Debortoli et al. 2017) as well as over the entire Amazon Basin (Marengo et al. 2001).

At local scales, the effects of deforestation were stronger during the onset of the rainy season than when the season was fully developed (Sumila et al. 2017). During the transition from the dry season to the wet season, most of the moisture provided to the atmosphere is from the local evapotranspiration and moisture convergence is small. The land cover heterogeneity of edges, between forest and cleared areas, also creates centers of strong atmospheric divergence and affects precipitation (Saad et al. 2010; Butt et al. 2011; Knox et al. 2011; Spracklen et al. 2012). Precipitation is altered through changes in the thermodynamic profile and the development of surface induced mesoscale circulation (Spracklen et al. 2012). Knox et al. (2015) found that the upwelling air generated at the deforested edge carries moisture, resulting in the formation of deep convective clouds. Consequently, higher rainfall is observed along forest edges, while in the interior of deforested areas, rainfall is lower. At larger scales, deforestation upwind of the upper Xingu Basin resulted in less water vapor to form precipitation over the Xingu Basin. The reduced moisture from deforestation affects rainfall totals in regions as far south as 15° to 20°S (Sumila et al. 2017; Arvor et al. 2017).

Climate modeling experiments have shown that preserving remnant native vegetation is essential to climate stability in the Amazon (Coe et al. 2013; Pires and Costa 2013). Silvério et al. (2015) found that land use transitions during the 2000s reduced contemporaneous

evapotranspiration in the Xingu region by 35 km^3 and warmed the land surface temperature by 0.3 °C. These feedbacks between land-cover changes and climate have the potential to reduce precipitation (Knox et al. 2015).

The abrupt change in rainfall in Xingu Basin that we observed after 1996 cannot be related exclusively to higher deforestation rates in Southern Amazon. Deforestation causes important reductions in evapotranspiration, but does not expressively decrease moisture convergence over the deforested area (Costa and Pires 2010). In this case, large-scale circulation patterns also induce cycles of wet and dry periods of 20 to 30 years duration in Amazon (Botta et al. 2002; Marengo 2009). The mid-1950s to late-1970s were a dry period in southern Amazon and were followed by higher rainfall rates until the end of the 1990s (Marengo 2009). In our case, we used a 40-year time series, which initially detected a positive phase in the interdecadal oscillation (1975–1990) and later a negative shift between mid-1990s and the late 2010s. Espinoza et al. (2009) indicated that mean rainfall in the Amazon Basin decreased during the 1975–2003 period, at an annual rate of − 0.32%. Marengo (2010) indicated a reduction of approximately 17% in southern Amazon rainfall. In these cases, the reductions were associated with an interdecadal oscillation of sea surface temperature, and consequently an alteration in the moisture transport towards the Amazon.

It is likely that global climate change will intensify these alterations in the future (Coe et al. 2013). Atmospheric greenhouse gases will raise temperatures and likely drought frequency and intensity (Malhi et al. 2008). Although climate projections for precipitation are highly variable (Almeida et al. 2016), several models indicate higher temperatures in the Xingu Basin (Vourlitis and da Rocha 2010; Lewis et al. 2011), as well as a decline in dry season rainfall and recurrent droughts (Zelazowski et al. 2011; Coe et al. 2013).

4.3 Deforestation and water yield

At the small scale of headwater watersheds, the approximately four times greater water yield from cropland catchments over multiple years caused by elimination of forest cover was similar to the patterns found by others in the Upper Xingu (Hayhoe et al. 2011; Dias et al. 2015; Riskin et al. 2017). In small watersheds, conversion of forest to croplands resulted in higher flows in both wet and dry season. Although seasonal variations in flow were greater in croplands, the overall magnitude of annual flow variation was small. This is because surface infiltrability and subsurface hydraulic conductivity are high in the deep and weathered Oxisols on which most cropping takes place (Scheffler et al. 2011). This generates deep and groundwater-dominated water flowpaths that do not produce overland flows and that stabilize streamflows across wet and dry seasons (Neill et al. 2013). In addition, the presence of more than 10,000 small impoundments constructed for roads and water supply to cattle when ranching dominated the Upper Xingu Basin (Macedo et al. 2013) likely decrease flow velocity and increase ET from water surfaces (Lehner et al. 2011). The relationship between land cover and stream flow and runoff in small watersheds in the upper Xingu Basin likely differs from that in other parts of the Amazon Basin on other soils. Small catchments in the Ji-Paraná Basin in Rondônia had a decreased capacity to regulate flows after deforestation and exhibited a greater difference between extreme flows, including both lower flows in dry season and higher flows in the rainy season (Rodriguez et al. 2010). Similar increases in water yield from deforested small watersheds have been found on soils with lower infiltrability and hydraulic conductivity in other parts of the Amazon (Biggs et al. 2006; Germer et al. 2010). Although soils play a very large role in controlling runoff processes (Bruijnzeel 2004) and much of the

Xingu Basin is underlain by permeable Oxisols (Neill et al. 2017), extrapolating results from a small number of headwater watersheds to the entire Xingu Basin is confounded by the presence of both less permeable soils and higher relief in the southern portion of the Basin where the headwaters of many Xingu tributaries are located, and large area of wetlands and flooded forest along the central floodplain but upstream of the river gauge at São Jose do Xingu.

4.4 Influences of rainfall changes in water yield

At the intermediate scale of the Ronuro Basin, lower rainfall was accompanied by a reduction in annual water yield from ~ 750 mm in the mid-1970s to ~ 650 mm after mid-1990s. The coherence among two independent sources of hydrological data (rainfall stations and Ronuros's gauge) indicated that although the dataset employed in this study might have considerable limitations, the alterations here observed were consistent. Furthermore, relatively low rates of deforestation that occurred in the Ronuro Basin during most of measurement period suggested that this trend was caused primarily by changes to climate and not by deforestation. Lack of discharge measurements of the Ronuro River after 2007 prevented further analysis after the period of high deforestation.

At the scale of the upper Xingu Basin, no alterations were observed in the Xingu River water yield. According to Coe et al. (2009) and Panday et al. (2015), the impacts of decreased rainfall were offset by increased water yield resultant of deforestation in the late-2000s. These authors performed modeling studies in the whole Xingu Basin (510,000 km^2) based on a modeling, ground, and satellite data analysis. Panday et al. (2015) suggested that climate variations accounted for 14% decrease in annual discharge, while deforestation caused a 6% increase in annual discharge. Such reduction in discharge resulted from a combined decrease in rainfall and increase in ET. Stickler et al. (2013) argued that in the absence of indirect effects caused by deforestation in the entire Amazon region (i.e., through changes to rainfall), discharge in the Xingu river Basin increased up to 12%. When indirect effects were considered, deforestation of the Amazon region inhibited rainfall within the Xingu Basin, counterbalancing declines in ET and decreasing discharge by 6–36%. Coe et al. (2009) indicated that with extensive deforestation (> 30% of the Amazon Basin), atmospheric feedbacks are not limited to those Basins where deforestation has occurred, but are spread unevenly throughout the entire Amazon by atmospheric circulation. In this scenario, the Xingu River would have a − 15% precipitation decrease caused by the regional atmospheric changes, and an 11% decrease in Xingu discharge (Coe et al. 2009). The current level of deforestation in the Xingu Basin has influenced river flow regulation at the local scale, resulting in increased river runoff and greater differences between dry and wet season water yield. At the larger scale, increased deforestation and reductions in rainfall had opposite effects on water yield, so decreased river flow caused by rainfall reduction was counteracted by increased water yield induced by deforestation.

Another aspect that should be considered when evaluating water availability in large-scale Basins is the potential effects of secondary growth under climate and land use change. Using a hydrological model driven by different climate and land use scenarios, Von Randow et al. (2019) observed that when only deforestation scenarios are included, the effects of climate change in water yield are weakened. But when secondary growth is also considered, the effects of climate change are enhanced. Considering that secondary growth accounts for an important portion of deforested vegetations in the Amazon (Aragão et al. 2014), better accounting for the effects of regrowing forest in water and energy balance should be considered in future studies.

5 Conclusions

During the last 40 years, the mean annual rainfall decreased by 245 mm year^{-1}, the greatest portion of which occurred after 1995. A reduction in the number of days with rain coincided with high rates of deforestation across the entire southeast Amazon, during the 1990s. Although there is evidence from other places that links rainfall patterns and the land use changes, we could not attribute these changes in the Xingu Basin exclusively to deforestation. Rainfall alterations are also related to decadal oscillations in sea surface temperature between tropical and subtropical Atlantic and the Pacific oceans. The water yield of Xingu river did not significantly change in the period evaluated. This is because of the offsetting effects of increased water yield from deforestation and reductions related to rainfall. The maintenance of high-quality and long-term rainfall and stream gauging stations distributed over large areas in the relatively remote Amazon Basin remains an important barrier to detecting land use-induced changes to the hydrological cycle and validating changes projected by earth system models. For the Xingu Basin, despite the existence of distributed rainfall measurement stations, a small proportion (6 out of 59) met rigorous criteria for data quality and completeness. But for these stations the good long-term records, the recurrent downward trend observed in all the six stations was strong evidence of long-term rainfall reductions.

In this study, the trends in rainfall and water yield were defined by a well stablished time series analysis. The Mann-Kendal and Pettitt analyses have been successfully employed in Amazon basin hydro-climatological studies (Marengo 2009; Rodriguez et al. 2010). On the other hand, they are not able to separate anthropic induced changes from those related to climate variability. In future studies, high-quality checked data, as the one presented here, could be analyzed with more robust techniques, such as model simulations (Stickler et al. 2013; Panday et al. 2015), or methods like the Tomer and Schilling framework (Tomer and Schilling 2009), the elasticity-based method (Schaake, 1990), and the decomposition of Budyko-type curve method (Wang and Hejazi 2011). These techniques were developed to address both the effects of climate variability and human activities on streamflow.

Funding information The Center of Nuclear Energy in Agriculture, the Inter-Institutional Graduate Program in Applied Ecology (ESALQ/CENA-USP), the Coordination for the Improvement of Higher Education Personnel (CAPES), and the São Paulo Research Foundation gave financial support (Proj. numbers 2013/20377-1 and 2013/50180-5) and NSF EAR 1739724.

References

Almeida CT, Oliveira-Júnior JF, Delgado RC et al (2016) Spatiotemporal rainfall and temperature trends throughout the Brazilian Legal Amazon, 1973-2013. Int J Climatol 37:2013. https://doi.org/10.1002/joc.4831

Aragão LEOC, Poulter B, Barlow JB et al (2014) Environmental change and the carbon balance of Amazonian forests. Biol Rev 89:913. https://doi.org/10.1111/brv.12088

Arvor D, Jonathan M, Meirelles MSP et al (2011) Classification of MODIS EVI time series for crop mapping in the state of Mato Grosso, Brazil. Int J Remote Sens 32:7847–7871. https://doi.org/10.1080/01431161.2010.531783

Arvor D, Dubreuil V, Ronchail J et al (2014) Spatial patterns of rainfall regimes related to levels of double cropping agriculture systems in Mato Grosso (Brazil). Int J Climatol 34:2622–2633. https://doi.org/10.1002/joc.3863

Arvor D, Funatsu BM, Michot V, Dubreui V (2017) Monitoring rainfall patterns in the southern amazon with PERSIANN-CDR data: long-term characteristics and trends. Remote Sens 9:889. https://doi.org/10.3390/rs9090889

Biggs TW, Dunne T, Muraoka T (2006) Transport of water, solutes and nutrients from a pasture hillslope, southwestern Brazilian Amazon. Hydrol Process 20:2527. https://doi.org/10.1002/hyp.6214

Botta A, Ramankutty N, Foley JA (2002) Long-term variations of climate and carbon fluxes over the Amazon basin. Geophys Res Lett 29:33-1. https://doi.org/10.1029/2001GL013607

Bruijnzeel LA (2004) Hydrological functions of tropical forests: not seeing the soil for the trees? Agric Ecosyst Environ 104:185

Butt N, De Oliveira PA, Costa MH (2011) Evidence that deforestation affects the onset of the rainy season in Rondonia, Brazil. J Geophys Res Atmos 116:2–9. https://doi.org/10.1029/2010JD015174

Coe MT, Costa MH, Soares-Filho BS (2009) The influence of historical and potential future deforestation on the stream flow of the Amazon River - land surface processes and atmospheric feedbacks. J Hydrol 369:165–174. https://doi.org/10.1016/j.jhydrol.2009.02.043

Coe MT, Latrubesse EM, Ferreira ME, Amsler ML (2011) The effects of deforestation and climate variability on the streamflow of the Araguaia River, Brazil. Biogeochemistry 105:119. https://doi.org/10.1007/s10533-011-9582-2

Coe MT, Marthews TR, Costa MH et al (2013) Deforestation and climate feedbacks threaten the ecological integrity of south-southeastern Amazonia. Philos Trans R Soc Lond Ser B Biol Sci 368:20120155. https://doi.org/10.1098/rstb.2012.0155

Coe MT, Macedo MN, Brando PM et al (2016) The hydrology and energy balance of the Amazon Basin. Springer, Berlin Heidelberg, pp 35–53

Costa MH, Foley JA (1997) Water balance of the Amazon Basin: dependence on vegetation cover and canopy conductance. J Geophys Res Atmos 102:23973–23989. https://doi.org/10.1029/97JD01865

Costa MH, Pires GF (2010) Effects of Amazon and Central Brazil deforestation scenarios on the duration of the dry season in the arc of deforestation. Int J Climatol 30:1970–1979. https://doi.org/10.1002/joc.2048

Costa MH, Botta A, Cardille JA (2003) Effects of large-scale changes in land cover on the discharge of the Tocantins River, Southeastern Amazonia. J Hydrol 283:206–217. https://doi.org/10.1016/S0022-1694(03)00267-1

da Rocha H, Goulden M, Miller SD et al (2004) Seasonality of water and heat fluxes over a tropical forest in eastern Amazonia. Ecol Appl 14:S22–S32. https://doi.org/10.1890/02-6001

Debortoli SN, Dubreuil V, Funatsu B et al (2015) Rainfall patterns in the Southern Amazon: a chronological perspective (1971-2010). Clim Chang 132:251–264. https://doi.org/10.1007/s10584-015-1415-1

Debortoli NS, Dubreuil V, Hirota M et al (2017) Detecting deforestation impacts in Southern Amazonia rainfall using rain gauges. Int J Climatol 37:2889. https://doi.org/10.1002/joc.4886

DeFries R, Herold M, Verchot L et al (2013) Export-oriented deforestation in Mato Grosso: harbinger or exception for other tropical forests? Philos Trans R Soc B Biol Sci 368:20120173–20120173. https://doi.org/10.1098/rstb.2012.0173

Delahaye F, Kirstetter PE, Dubreuil V et al (2015) A consistent gauge database for daily rainfall analysis over the Legal Brazilian Amazon. J Hydrol 527:292. https://doi.org/10.1016/j.jhydrol.2015.04.012

Dias LCP, Macedo MN, Costa MH et al (2015) Effects of land cover change on evapotranspiration and streamflow of small catchments in the Upper Xingu River Basin, Central Brazil. J Hydrol Reg Stud 4:108–122. https://doi.org/10.1016/j.ejrh.2015.05.010

Fu R, Li W (2004) The influence of the land surface on the transition from dry to wet season in Amazonia. Theor Appl Climatol 78:97–110. https://doi.org/10.1007/s00704-004-0046-7

Garcia AS, Sawakuchi HO, Ferreira ME, Ballester MVR (2017) Landscape changes in a neotropical forest-savanna ecotone zone in central Brazil: the role of protected areas in the maintenance of native vegetation. J Environ Manag 187:16. https://doi.org/10.1016/j.jenvman.2016.11.010

Germer S, Neill C, Krusche AV, Elsenbeer H (2010) Influence of land-use change on near-surface hydrological processes: undisturbed forest to pasture. J Hydrol 380:473. https://doi.org/10.1016/j.jhydrol.2009.11.022

Hayhoe SJ, Neill C, Porder S et al (2011) Conversion to soy on the Amazonian agricultural frontier increases streamflow without affecting stormflow dynamics. Glob Chang Biol 17:1821–1833. https://doi.org/10.1111/j.1365-2486.2011.02392.x

Júnior JLS, Tomasella J, Rodriguez DA (2015) Impacts of future climatic and land cover changes on the hydrological regime of the Madeira River basin. Clim Chang 129:117. https://doi.org/10.1007/s10584-015-1338-x

Kendall MG (1975) Rank correlation methods

Knox R, Bisht G, Wang J et al (2011) Precipitation variability over the forest-to-nonforest transition in southwestern Amazonia. J Clim 24:2368–2377. https://doi.org/10.1175/2010JCLI3815.1

Knox RG, Longo M, Swann ALS et al (2015) Hydrometeorological effects of historical land-conversion in an ecosystem-atmosphere model of Northern South America. Hydrol Earth Syst Sci 19:241
Lathuillière MJ, Johnson MS, Galford GL, Couto EG (2014) Environmental footprints show China and Europe's evolving resource appropriation for soybean production in Mato Grosso, Brazil. Environ Res Lett 9. https://doi.org/10.1088/1748-9326/9/7/074001
Lehner B, Liermann CR, Revenga C et al (2011) High-resolution mapping of the world's reservoirs and dams for sustainable river-flow management. Front Ecol Environ 9:494–502. https://doi.org/10.1890/100125
Leite-Filho AT, de Sousa Pontes VY, Costa MH (2019) Effects of deforestation on the onset of the rainy season and the duration of dry spells in Southern Amazonia. J Geophys Res Atmos https://doi.org/10.1029/2018JD029537
Levy MC, Lopes AV, Cohn A et al (2018) Land use change increases streamflow across the arc of deforestation in Brazil. Geophys Res Lett 45:3520. https://doi.org/10.1002/2017GL076526
Lewis SL, Brando PM, Phillips OL et al (2011) The 2010 Amazon drought. Science 331:554. https://doi.org/10.1126/science.1200807
Macedo MN, DeFries RS, Morton DC et al (2012) Decoupling of deforestation and soy production in the southern Amazon during the late 2000s. Proc Natl Acad Sci 109:1341–1346. https://doi.org/10.1073/pnas.1111374109
Macedo MN, Coe MT, DeFries R et al (2013) Land-use-driven stream warming in southeastern Amazonia. Philos Trans R Soc Lond Ser B Biol Sci 368:20120153
Makarieva AM, Gorshkov VG, Sheil D et al (2013) Where do winds come from? A new theory on how water vapor condensation influences atmospheric pressure and dynamics. Atmos Chem Phys 13:1039–1056. https://doi.org/10.5194/acp-13-1039-2013
Malhi Y, Roberts JT, Betts RA et al (2008) Climate change, deforestation, and the fate of the Amazon. Science 319:169–172. https://doi.org/10.1126/science.1146961
Mann HB (1945) Nonparametric tests against trend. Econometrica 13:245. https://doi.org/10.2307/1907187
Marengo JA (2009) Long-term trends and cycles in the hydrometeorology of the Amazon basin since the late 1920s. Hydrol Process 23:3236. https://doi.org/10.1002/hyp.7396
Marengo JA, Liebmann B, Kousky VE et al (2001) Onset anf end of the rainy season in the Brazilian Amazon Basin. J Clim 14:833–852
Marengo JA, Tomasella J, Alves LM et al (2011) The drought of 2010 in the context of historical droughts in the Amazon region. Geophys Res Lett 38. https://doi.org/10.1029/2011GL047436
Morton DC, DeFries RS, Shimabukuro YE et al (2006) Cropland expansion changes deforestation dynamics in the southern Brazilian Amazon. Proc Natl Acad Sci. https://doi.org/10.1073/pnas.0606377103
Negri AJ, Anagnostou EN, Adler RF et al (2000) A 10-yr climatology of Amazonian rainfall derived from passive microwave satellite observations. J Appl Meteorol 39:42–56. https://doi.org/10.1175/1520-0450(2000)039<0042:AYCOAR>2.0.CO;2
Neill C, Coe MT, Riskin SH et al (2013) Watershed responses to Amazon soya bean cropland expansion and intensification. Philos Trans R Soc B Biol Sci 368:20120425. https://doi.org/10.1098/rstb.2012.0425
Neill C, Jankowski K, Brando PM, et al (2017) Surprisingly modest water quality impacts from expansion and intensification of large-scale commercial agriculture in the Brazilian Amazon-Cerrado Region. Trop Conserv Sci https://doi.org/10.1177/1940082917720669
Panday PK, Coe MT, Macedo MN et al (2015) Deforestation offsets water balance changes due to climate variability in the Xingu River in eastern Amazonia. J Hydrol 523:822–829. https://doi.org/10.1016/j.jhydrol.2015.02.018
Pettitt AN (1979) A non-parametric approach to the change-point problem. Appl Stat 28:126. https://doi.org/10.2307/2346729
Pfaff A, Robalino J, Walker R et al (2007) Road investments, spatial spillovers, and deforestation in the Brazilian Amazon. J Reg Sci 47:109. https://doi.org/10.1111/j.1467-9787.2007.00502.x
Pires GF, Costa MH (2013) Deforestation causes different subregional effects on the Amazon bioclimatic equilibrium. Geophys Res Lett 40:3618. https://doi.org/10.1002/grl.50570
Riskin SH, Neill C, Jankowski K et al (2017) Solute and sediment export from Amazon forest and soybean headwater streams. Ecol Appl 27:193–207. https://doi.org/10.1002/eap.1428
Rodriguez DA, Tomasella J, Linhares C (2010) Is the forest conversion to pasture affecting the hydrological response of Amazonian catchments? Signals in the Ji-Paran?? Basin. Hydrol Process 24:1254–1269
Saad SI, da Rocha HR, Silva Dias MAF et al (2010) Can the deforestation breeze change the rainfall in Amazonia? A case study for the BR-163 highway region. Earth Interact 14:1–25. https://doi.org/10.1175/2010EI351.1
Scheffler R, Neill C, Krusche AV, Elsenbeer H (2011) Soil hydraulic response to land-use change associated with the recent soybean expansion at the Amazon agricultural frontier. Agric Ecosyst Environ 144:281. https://doi.org/10.1016/j.agee.2011.08.016

Schubert SD, Suarez MJ, Pegion PJ et al (2004) Causes of long-term drought in the U.S. Great Plains. J Clim 17: 485–503. https://doi.org/10.1175/1520-0442(2004)017<0485:COLDIT>2.0.CO;2
Sen PK (1968) Estimates of the regression coefficient based on Kendall's tau. J Am Stat Assoc 63:1379. https://doi.org/10.1080/01621459.1968.10480934
Silvério DV, Brando PM, Macedo MN et al (2015) Agricultural expansion dominates climate changes in southeastern Amazonia: the overlooked non-GHG forcing. Environ Res Lett 10:104015. https://doi.org/10.1088/1748-9326/10/10/104015
Siqueira JR, Toledo Machado LA, Siqueira JR, Machado LAT (2004) Influence of the frontal systems on the day-to-day convection variability over South America. J Clim 17:1754–1766. https://doi.org/10.1175/1520-0442(2004)017<1754:IOTFSO>2.0.CO;2
Spera SA, Galford GL, Coe MT et al (2016) Land-use change affects water recycling in Brazil's last agricultural frontier. Glob Chang Biol 22:3405. https://doi.org/10.1111/gcb.13298
Spracklen DV, Arnold SR, Taylor CM (2012) Observations of increased tropical rainfall preceded by air passage over forests. Nature 489:282–285. https://doi.org/10.1038/nature11390
Stickler CM, Coe MT, Costa MH et al (2013) Dependence of hydropower energy generation on forests in the Amazon Basin at local and regional scales. Proc Natl Acad Sci U S A 110:9601–9606. https://doi.org/10.1073/pnas.1215331110
Sumila TCA, Pires GF, Fontes VC, Costa MH (2017) Sources of water vapor to economically relevant regions in Amazonia and the effect of deforestation. J Hydrometeorol. https://doi.org/10.1175/JHM-D-16-0133.1
Tomer MD, Schilling KE (2009) A simple approach to distinguish land-use and climate-change effects on watershed hydrology. J Hydrol 376:24. https://doi.org/10.1016/j.jhydrol.2009.07.029
Von Randow RCS, Rodriguez DA, Tomasella J et al (2019) Response of the river discharge in the Tocantins River Basin, Brazil, to environmental changes and the associated effects on the energy potential. Reg Environ Chang 19:193. https://doi.org/10.1007/s10113-018-1396-5
Vourlitis G, da Rocha H (2010) Flux dynamics in the Cerrado and Cerrado–Forest transition of Brazil. In: Ecosystem Function in Savannas. CRC Press, pp 97–116
Wang D, Hejazi M (2011) Quantifying the relative contribution of the climate and direct human impacts on mean annual streamflow in the contiguous United States. Water Resour Res 47. https://doi.org/10.1029/2010WR010283
Wright JS, Fu R, Worden JR et al (2017) Rainforest-initiated wet season onset over the southern Amazon. Proc Natl Acad Sci 114:8481. https://doi.org/10.1073/pnas.1621516114
Yin L, Fu R, Zhang YF et al (2014) What controls the interannual variation of the wet season onsets over the amazon? J Geophys Res 119:2314. https://doi.org/10.1002/2013JD021349
Yue S, Pilon P, Phinney B, Cavadias G (2002) The influence of autocorrelation on the ability to detect trend in hydrological series. Hydrol Process 16:1807. https://doi.org/10.1002/hyp.1095
Zelazowski P, Malhi Y, Huntingford C et al (2011) Changes in the potential distribution of humid tropical forests on a warmer planet. Philos Trans R Soc A Math Phys Eng Sci 369:137–160. https://doi.org/10.1098/rsta.2010.0238
Zhang K, Kimball JS, Nemani RR et al (2015) Vegetation greening and climate change promote multidecadal rises of global land evapotranspiration. Sci Rep 5:15956. https://doi.org/10.1038/srep15956

Affiliations

Rodnei Rizzo[1] · Andrea S. Garcia[1] · Vívian M. de F. N. Vilela[1] · Maria Victoria R. Ballester[1] · Christopher Neill[2] · Daniel C. Victoria[3] · Humberto R. da Rocha[4] · Michael T. Coe[2]

[1] Environmental Analysis and Geoprocessing Laboratory, Center for Nuclear Energy in Agriculture, University of São Paulo, Av. Centenário, 303, Piracicaba, SP 13416-000, Brazil

[2] Woods Hole Research Center, 149 Woods Hole Road, Falmouth, MA 02540, USA

[3] Embrapa Agricultural Informatics, Brazilian Agricultural Research Corporation, Campinas, SP 13070, Brazil

[4] Instituto de Astronomia, Geofísica e Ciências Atmosféricas, Universidade de São Paulo, São Paulo, Brazil